

EFFECT OF SHOCK-WAVE EXIT ANGLE ON A FREE SURFACE ON
FRACTURE FORMATION IN METALS

V. K. Golubev, S. A. Novikov,
L. M. Sinitsyna, N. A. Yukina

UDC 539.4

Fracture destruction of materials upon loading of plates by flat explosive charges was studied in [1-3]. The experimental technique used therein can be modified by using specimens in the form of a wedge [4]. If this is done the critical loading conditions leading to macroscopic fracture of materials can be determined in a single experiment, as can the conditions corresponding to generation of fracture microdefects within the material. In addition, by varying the value of the wedge angle and the direction of shock loading, information can be obtained on the effect of shock wave exit angle on the free surface upon critical fracture formation conditions in the given material.

The present study will present preliminary results of an investigation of type AD1 aluminum, AMg6 aluminum alloy, M1 copper, and St. 3 steel. Specimens were cut from large-diameter bars in the form of wedges with various wedge angles γ . The transverse and longitudinal dimensions of the specimens were selected sufficiently large to eliminate the effects of lateral deloading and the initial nonstationary loading zone upon the fracture formation process. To remove internal stresses, the AD1 and AMg6 specimens were annealed at 350°C and the M1 and St. 3 specimens at 600°C for 1 h. The experimental configuration, explosive parameters, and shock adiabats used for numerical calculations were described in [3]. The value of the shock wave exit angle on the free surface was determined as follows: $\alpha = \beta \pm \gamma$, where $\beta = \arcsin(c_0/D)$, and c_0 is the coefficient of the linear D-u relationship, D being the explosive detonation rate, and the plus and minus signs correspond to loading from the peak or the base of the wedge. The specimen depth at the point of formation of the macroscopic fracture h_2 was determined. The h_2 value was measured along the normal to the loaded wedge surface. The experimental results obtained are presented in Fig. 1 in the form of dimensionless critical specimen thicknesses corresponding to fracture formation, $\bar{h}_* = h_2/h_1$, where h_1 is the explosive charge thickness, versus exit angle α . The points in Fig. 1 correspond to the following metals: 1, 2, AD1 aluminum, $h_1 = 0.78$ and 0.5 mm; 3, 4, copper, $h_1 = 0.6$ and 0.75 mm; 5-7, St. 3 steel, $h_1 = 2.6, 2.0,$ and 1.35 mm; 8, AMg6 alloy, $h_1 = 0.78$ mm; 9, AD1 aluminum, $h_1 = 0.47$ mm [3]; 10, copper, $h_1 = 0.65$ mm [3]. Photographs of some of the specimens tested are presented in Fig. 2 (a, AMg6 alloy; b, AD1 aluminum, $h_1 = 0.78$ mm) and Fig. 3 (St. 3 steel, a, $\alpha = 24^\circ$, b, $\alpha = 48^\circ$, $h_1 = 2.0$ mm).

For all materials tested, there was a tendency toward reduction in \bar{h}_* with increase in angle α . This, in turn, indicates that an increase in angle α leads to an increase in critical pressure p_* in the shock wave required for fracture formation. We will attempt to esti-

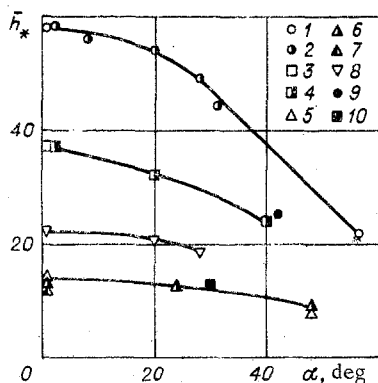


Fig. 1

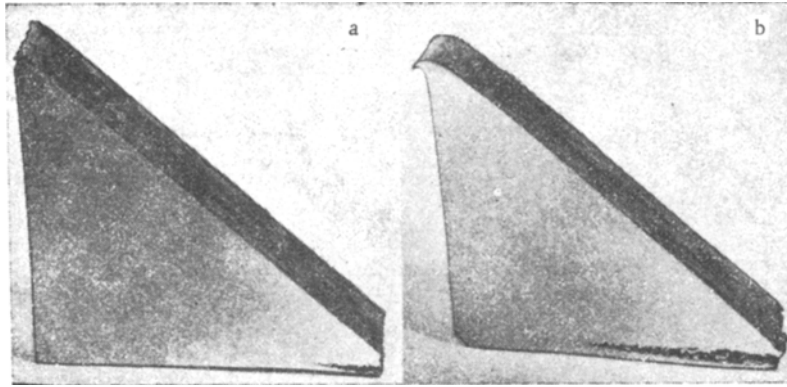


Fig. 2



Fig. 3

mate the pressure p produced in the shock wave excited by the detonation of the explosive layer as a function of the depth to which it penetrates into metal h . In the dimensionless coordinates $\bar{p} = p/p_0$, where $p_0 = \rho D^2/4$ is the Jouguet pressure, and $\bar{h} = h/h_1$, Fig. 4 presents the data required for such an estimate. Curves 1 and 2 are results of hydrodynamic calculations of shock wave attenuation in steel and aluminum [3], curve 3 is experimental results for St. 3 steel [2], while curve 4 is experimental results for the aluminum alloy AMts [1]. The lower \bar{h} scale is for aluminum, the upper one, for steel. While in the case of aluminum the hydrodynamic calculation gives a satisfactory description of attenuation for $\bar{h} < 20$, for St. 3 steel, which has very high shear strength, there is significant divergence between calculated and experimental results. The experimental results 3 and 4 over the ranges \bar{h} (1-7) and (1-30) can be approximated by monotonically decreasing functions $\bar{p}(\bar{h})$ 5 and 6 respectively. We will extrapolate these curves to values of $\bar{h} = 15$ and 60 for steel and aluminum. This will require certain further assumptions. First, the true function $\bar{p}(\bar{h})$ should show a more significant decrease than the hydrodynamic calculation, i.e., the distance between the curves should increase with increase in \bar{h} . Second, we assume that curves 5 and 6 pass through the ranges 7 and 8, the upper limits of which correspond to critical fracture formation conditions for St. 3 steel and AD1 aluminum under conditions of normal shock wave incidence on the free surface, while the lower limits are conditions for formation of fracture microdefects in the materials. For copper, the hydrodynamic approximation calculation of $\bar{p}(\bar{h})$ actually coincides with the calculated dependence for steel. Considering the lower shear strength of copper, it is acceptable that the $\bar{p}(\bar{h})$ curve for copper will be located somewhat above curve 5 for steel,

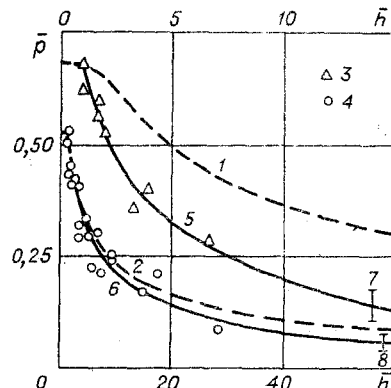


Fig. 4

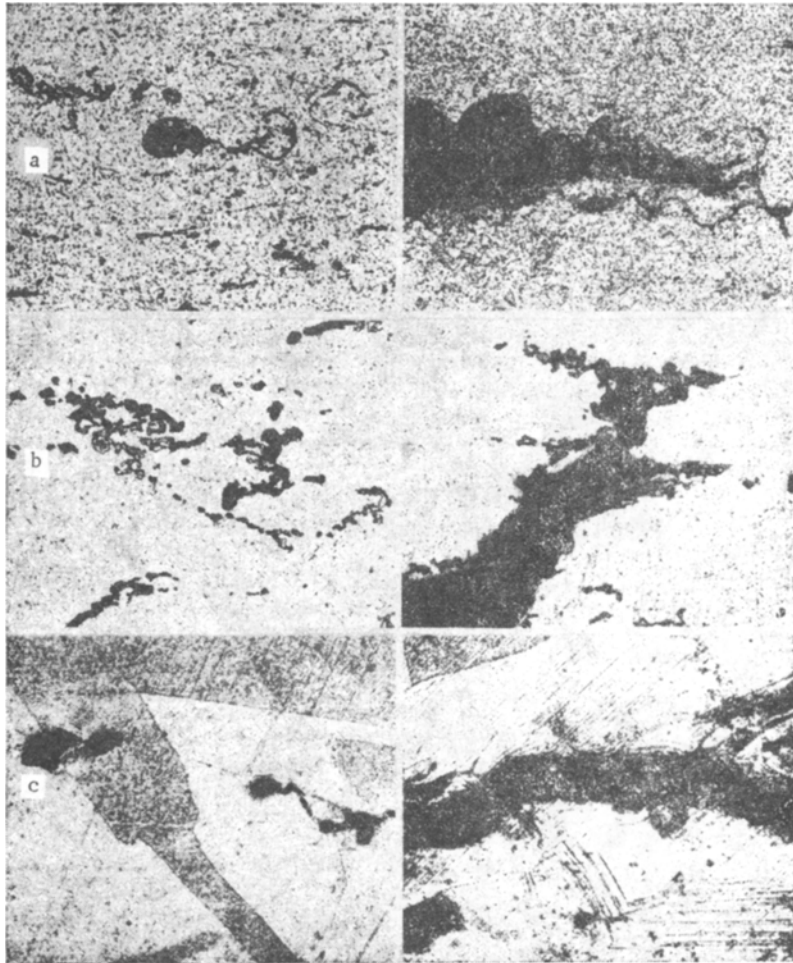


Fig. 5

and consideration of its monotonicity and passage through a similar critical value range will allow comparative estimates of p_* for various angles α .

Calculations of the effect of angle α on p_* revealed that an increase in α from 0 to 56° leads to an increase in p_* for aluminum from 1.4 to 3.0 GPa. For the aluminum alloy AMg6 the p_* value at $\alpha = 0^\circ$ should be somewhat less than 3.0 GPa (shock wave attenuation in the harder alloy AMg6 must be higher than in the plastic AMts), and p_* increases to 3.5 GPa at $\alpha = 28^\circ$. For St. 3 steel, increase in α from 0 to 48° leads to an increase in p_* from 3.3 to 5.0 GPa, while for copper, increase in α from 0 to 40° leads to increase in p_* from 3.0 to 3.9 GPa.

A metallographic analysis of the character of fracture destruction of the metals studied was performed. Figure 5 (200 \times magnification) shows a view of the microdefects generated (left-hand views) and the initial stage of macroscopic fracture formation (right-hand views) in aluminum (a), AMg6 alloy (b), and copper (c). Results for St. 3 steel are shown in Fig. 6: a, intense twinning in ferrite grains in a thin (~ 1 mm at $h_1 = 2.0$ mm) layer at the loading surface, $\times 500$; b, microcracks being formed, $\times 500$; c, initial stage of macrofracture formation, $\times 200$.

Figure 7 shows results of Vickers hardness determinations of several of the metals tested: 1, aluminum, $h_1 = 0.78$ mm; 2, AMg6 alloy, $h_1 = 0.78$ mm; 3, copper, $h_1 = 0.6$ mm; 4, St. 3 steel, $h_1 = 2.0$ mm. Measurements were performed with a 50-N loading. At least seven impressions were measured at each point. In their original state, the specimen materials showed hardnesses of 19.5, 82, 49, and 124 GPa, respectively.

We will note some unique features of the results obtained. There is a clear tendency to increase in the critical pressure in the shock wave required to produce fracture in the metals studied. To explain this phenomenon, it is desirable to study the effect of shock-wave exit angle on the critical conditions for generation of fracture microdefects, and to

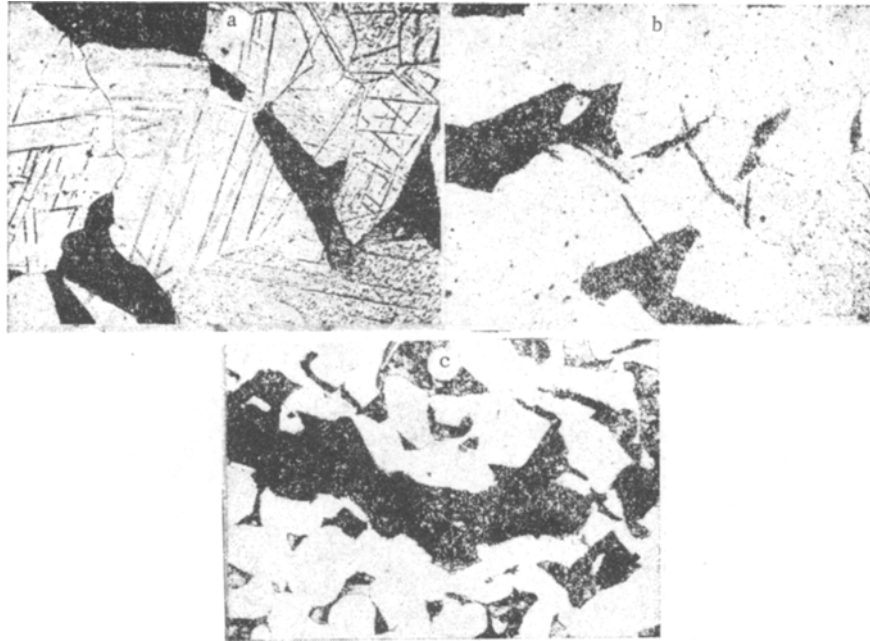


Fig. 6

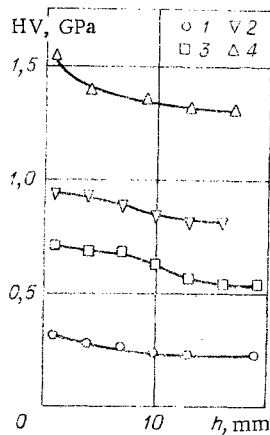


Fig. 7

use the results obtained for a calculated simulation of the oblique loading process, considering the real elastoplastic properties of the materials and the kinetics of microdefect accumulation and its effect on the character of wave processes in the failing material.

Of definite interest is the question of the effect of alloying on the fracture strength of the materials. Figure 2 shows views of AD1 aluminum and AMg6 aluminum alloy specimens (main alloying component magnesium) which had been loaded by explosions of planar charges of identical thicknesses. It is evident that the two materials have significantly different resistance to macroscopic fracture destruction, as was also observed in [5], while generation of microdefects in both materials takes place at approximately the same loading level (~ 1.0 GPa).

Thermal processing also has a significant effect on resistance of the metals to fracture destruction. As an example, Fig. 1 shows points 9, 10, from [3], where the specimens had no preliminary thermal processing. Calculations show that the thermal processing performed led to a reduction in p_* for aluminum and copper of 25 and 40%, respectively.

The results of the metallographic analysis indicate that fracture formation in aluminum, AMg6 alloy, and copper (Fig. 5) has a viscous character. The microdefects are pores of arbitrary form and small viscous microcracks, while in [6] the microdefects generated in aluminum and copper had the form of spherical pores. In the alloy AMg6 the microdefects were formed

at accumulations of inclusions, while in aluminum and copper they occurred at random. Merger of a large number of microdefects leads to formation of viscous macrocracks. The intense ferrite twinning zone observed in St. 3 steel (Fig. 6) is produced by a reversible phase transition of α -iron to the ϵ -phase at pressures above 13 GPa. Commencement of fracture destruction in St. 3 steel in the form of microcracks is of a brittle character, while development of the macrocrack occurs in a more viscous manner, as was also observed in [7].

The hardness measurements indicate that shock hardening of the materials is generally insignificant. For example, in the case of copper at a pressure of ~ 15 GPa, close to the pressure on the loading surface, according to an analysis of a large number of experimental studies performed in [8], the hardness increases to 0.9–1.0 GPa, while in the present study a value of 0.7 GPa was found. Similar differences were found for the other metals. Apparently this can be explained by the fact that in the present study massive specimens were loaded by thin planar explosive charges, which are relatively low-intensity and localized loading sources. Therefore the deformation produced by settling and bending of the metals was minimal, while the contribution of these factors to explosive hardening is apparently quite significant.

LITERATURE CITED

1. E. V. Menteshov, V. P. Ratnikov, et al., "Action of a planar explosive charge on an aluminum plate," *Fiz. Goreniya Vzryva*, No. 2 (1967).
2. A. P. Rybakov, E. V. Menteshov, and V. P. Shavkov, "Action of a planar explosive charge on metal plates," *Fiz. Goreniya Vzryva*, No. 1 (1968).
3. V. K. Golubev, S. A. Novikov, and L. M. Sinitsyna, "Material destruction by explosive loading with planar charges," *Zh. Prikl. Mekh. Tekh. Fiz.*, No. 2 (1981).
4. V. K. Golubev, S. A. Novikov, and L. M. Sinitsyna, "A method for fracture testing materials," *Otkrytiya, Izobret., Promyshl. Obraztsy. Tov. Zn.*, No. 34 (1981).
5. V. K. Golubev, S. A. Novikov, et al., "Effect of temperature on critical conditions for fracture destruction of metals," *Zh. Prikl. Mekh. Tekh. Fiz.*, No. 4 (1980).
6. T. W. Barbee, L. Seaman, et al., "Dynamic fracture criteria for ductile and brittle metals," *J. Mater.*, 7, No. 3 (1972).
7. V. K. Golubev, S. A. Novikov, et al., "Fracture failure mechanisms in St. 3 and 12Kh18-Ni0T steels in the temperature range -196 to 800°C ," *Probl. Prochn.*, No. 5 (1981).
8. A. A. Deribas, *The Physics of Explosive Hardening and Welding* [in Russian], Nauka, Novosibirsk (1980).